BIOCHEMISTRY
including biophysical chemistry & molecular biology

Article

pubs.acs.org/biochemistry

Thermodynamics of Insertion and Self-Association of a Transmembrane Helix: A Lipophobic Interaction by Phosphatidylethanolamine

Yoshiaki Yano, Arisa Yamamoto, Mai Ogura, and Katsumi Matsuzaki*

Graduate School of Pharmaceutical Sciences, Kyoto University, Sakyo-ku, Kyoto 606-8501, Japan

Supporting Information

ABSTRACT: Thermodynamic parameters for the insertion and self-association of transmembrane helices are important for understanding the folding of helical membrane proteins. The lipid composition of bilayers would significantly affect these fundamental processes, although how is not well understood. Experimental systems using model transmembrane helices and lipid bilayers are useful for measuring and interpreting thermodynamic parameters (ΔG, ΔH, ΔS, and ΔC_p) for the processes. In this study, the effect of the charge, phase, acyl chain unsaturation, and lateral pressure profile of bilayers on the membrane partitioning of the transmembrane helix $(AALALAA)_3$ was examined. Furthermore, the effect of 1-palmitoyl-2-oleoyl-*sn*-glycero-3-phosphatidylethanolamine (POPE) on the thermodynamics for insertion and self-association of the helix in host membranes composed of 1-palmitoyl-2-oleoyl-*sn*-glycero-3-phosphatidylcholine (POPC) was investigated in detail. Interbilayer transfer of the helix monomer from POPC to POPC/POPE (1/1) bilayers was unfavorable (ΔG = +4.5 ± 2.9 kJ mol^{-1} at 35 °C) due to an increase in enthalpy (ΔH = +31.1 ± 2.1 kJ mol^{-1}). On the other hand, antiparallel dimerization of the helices in POPC/POPE (1/1) bilayers was enhanced compared with that in POPC bilayers ($\Delta\Delta G$ = −4.9 ± 0.2 kJ mol^{-1} at 35 °C) due to a decrease in enthalpy ($\Delta\Delta H$ = −33.2 ± 1.5 kJ mol^{-1}). A greater thickness of POPC/POPE bilayers only partially explained the observed effects. The residual effects could be related to changes in other physical properties such as higher lateral pressure in the hydrocarbon core in the PE-containing membrane. The origin of the enthalpy-driven "lipophobic" force that modulates the insertion and association of transmembrane helices will be discussed.

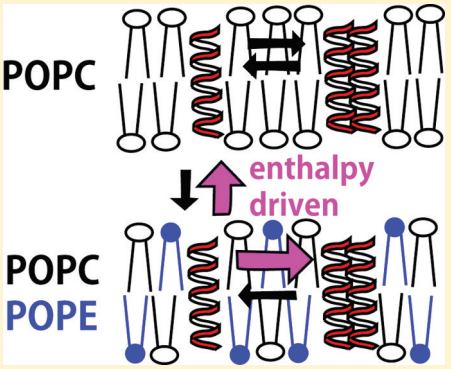

Integral membrane proteins are crucial to cellular functions such as transport, signal transduction, and energy conversion. However, the forces that determine the folding and stability of membrane proteins are not well understood compared with those for soluble proteins because of experimental limitations such as the insolubility of hydrophobic proteins and difficulties with protein-folding experiments.[1,2] Furthermore, the folding and function of a membrane protein are determined not only by the amino acid sequence of the protein but also by the physical properties of lipid bilayers surrounding the protein. Experiments using proteoliposomes have shown that activities of membrane proteins are often affected by lipid composition.[3,4] For example, nonbilayer-forming lipids such as phosphatidylethanolamine (PE) with a negative spontaneous curvature can alter the activities of a protein translocase,[5] ATPases,[6] and rhodopsin.[7] Both specific lipid−protein interactions and general changes in the physical properties of lipid bilayers are possible mechanisms for the effect. The general influence of nonbilayer lipids has often been ascribed to the modulation of conformational equilibria of proteins originating from a change in elastic curvature stress of the bilayer (or a change in lateral pressure profile),[7−9] although it has been difficult to directly measure forces that drive the folding of proteins in lipid bilayers.

In spite of the experimental limitations and mysterious effects of lipid composition, it is widely accepted that the folding of helical membrane proteins can be separated into two thermodynamically distinct stages. First, each hydrophobic domain forms a transmembrane helix, and the helices then interact to form a tertiary structure.[10,11] In the biosynthesis of membrane proteins, translocons are essential for effective integration and topology formation in lipid bilayers,[12] although even in the folding process mediated by translocons, the helices are considered to be in thermodynamic equilibrium with lipid bilayers.[13−15] A promising approach to elucidating the forces driving the folding of membrane proteins in the context of the thermodynamics of helix−helix, helix−lipid, and lipid−lipid interactions is the use of peptides forming transmembrane helices and lipid bilayers. A number of studies have investigated the insertion of helices and helix−helix interactions in membranes using specially designed hydrophobic peptides.[16,17] We have measured thermodynamic parameters for the self-association and intermembrane transfer of the completely hydrophobic transmembrane helix $(AALALAA)_3$.[18,19] The

Received: April 14, 2011
Revised: July 12, 2011
Published: July 13, 2011

sequence is devoid of motifs that drive oligomerization, such as GXXXG, leucine zipper motifs, and polar interactions. The membrane partitioning and self-association of even this "inert" transmembrane helix (hydrophobic length of 27−28.5 Å) was found to significantly depend on the hydrophobic thicknesses of bilayers (20−34 Å) composed of di-monounsaturated phosphatidylcholine (PC) lipids.

In this study, the effects of the charge, phase, acyl chain unsaturation, and lateral pressure profile of lipid bilayers on the membrane partitioning of $(AALALAA)_3$ were examined by monitoring the intervesicular transfer of the helix.[19,20] The analysis focused on the inhibitory effect of 1-palmitoyl-2-oleoyl-*sn*-glycero-3-phosphatidylethanoamine (POPE), which induces a higher lateral pressure in the hydrocarbon core region in the host membrane of 1-palmitoyl-2-oleoyl-*sn*-glycero-3-phosphatidylcholine (POPC). Fourier transform infrared-polarized attenuated total reflection (FTIR-PATR) spectroscopy was used to confirm the transmembrane orientation of the helix. Furthermore, fluorescence resonance energy transfer (FRET) experiments were performed to detect self-association of the helix, which was enhanced in PE-containing membranes. Thermodynamic parameters for membrane partitioning and self-association of the helix were obtained and compared with those in POPC bilayers. A "lipophobic" interaction on transmembrane helices will be discussed.

EXPERIMENTAL PROCEDURES

Materials. X-$(AALALAA)_3$-Y (X = 7-nitrobenz-2-oxa-1,3-diazole (NBD) and Y = NH_2 (**I**) or X = Ac and Y = $NHCH_2CH_2$−S-*N*-[4-[[4-(dimethylamino)phenyl]azo]-phenyl]-4′-maleimide (DABMI) (**II**)) was custom-made and characterized by the Peptide Institute (Minoh, Japan). The purity of the peptides was confirmed by reverse-phase high-performance liquid chromatography and ion-spray mass spectroscopy. Phospholipids were obtained from Avanti (Alabaster, AL). Spectrograde chloroform and methanol were products of Nacalai Tesque (Kyoto, Japan). The lipid was dissolved in chloroform, and its concentration was determined in triplicate by phosphorus analysis.[21] Lissamine Rhodamine B 1,2-dihexadecanol-*sn*-glycero-3-phosphatidylethanolamine, triethylammonium salt (Rh-PE), and *N*-(7-nitrobenz-2-oxa-1,3-diazol-4-yl)-1,2-dihexadecanoyl-*sn*-glycero-3-phosphoethanolamine, triethylammonium salt (NBD-PE), were obtained from Invitrogen (Carlsbad, CA). All other chemicals were of special grade and obtained from Wako (Tokyo, Japan).

FTIR-PATR Spectroscopy. Oriented films of lipid/peptide were prepared by uniformly spreading a 2,2,2-trifluoroethanol solution (0.1 mL) of 50 mM lipid/0.25 mM peptide on a germanium ATR plate (70 × 10 × 5 mm) followed by gradual evaporation of the solvent with N_2 gas. The last trace of the solvent was removed under vacuum overnight. The films were hydrated with a D_2O-soaked piece of filter paper put over the plate for 3 h at 25 °C. FTIR-PATR measurements were carried out as described in ref 18 on a BioRad FTS-3000MX spectrometer equipped with a Specac horizontal ATR attachment with an AgBr polarizer and a temperature controller. The dichroic ratio, R, defined by $\Delta A_{II}/\Delta A_{\perp}$, was calculated from the polarized spectra. The absorbance (ΔA) was obtained as the area for the amide I band. The subscripts II and ⊥ refer to polarized light with the electric vector parallel and perpendicular to the plane of incidence, respectively. The averaged helix orientation angle to bilayer normal, α, was calculated from R.[22]

$$\cos^2 \alpha = \frac{1}{3}\left(\frac{4}{3\cos^2 \theta - 1}\frac{R - 2.00}{R + 1.45} + 1\right) \quad (1)$$

We assumed a fixed angle (θ) of 35° between the helix axis and the transition moments for amide I bands.[22]

Preparation of Vesicles. Large unilamellar vesicles (LUVs) were prepared by an extrusion method using a buffer containing 10 mM Tris, 150 mM NaCl, and 1 mM EDTA (pH 7.4).[18] Freezing and thawing of multilamellar vesicles containing the peptides were avoided.

Intervesicular Transfer of Peptide. The intervesicular transfer of the peptide was determined by relief from FRET between the NBD-labeled peptide **I** and Rh-PE in donor vesicles upon transfer to acceptor vesicles without Rh-PE, as described elsewhere.[19] Donor POPC LUVs (200 μM) incorporating 0.5 mol % **I** and 2 mol % Rh-PE were mixed with an excess of acceptor LUVs (1 mM) composed of various phospholipids. Fluorescence emission spectra at 430−650 nm (excited at 450 nm) were measured on a Shimadzu RF-5300 spectrofluorometer (Kyoto, Japan). The efficiency of peptide transfer to the acceptor vesicle populations was determined by a decrease in sensitized fluorescence of Rh-PE at 590 nm (n = 2). After subtracting the contribution of directly excited Rh-PE fluorescence, the intensity of sensitized fluorescence of Rh-PE was obtained from a least-squares curve fitting using a linear combination of emission spectra of **I** and Rh-PE. The sensitized fluorescence of Rh-PE instead of the donor NBD fluorescence was used as an indicator of the transfer because the emission quantum yield and spectral shape of NBD depend on the lipid species in the acceptor vesicles. The sensitized fluorescence intensity of Rh-PE was confirmed to be proportional to the peptide concentration in the donor vesicles.[19] Therefore, $F_X(t)$ being sensitized rhodamine fluorescence at time t after mixing with acceptor vesicles, the amounts of the peptide in the donor and acceptor vesicles are simply proportional to $F_X(t)$ and $F_X(0) - F_X(t)$, respectively, because the fraction of the peptide in aqueous phase is negligible. The equilibrium peptide concentrations in the donor ($[P]_D$) and the acceptor ($[P]_A$) vesicles can be calculated as

$$[P]_D = \frac{F_X(\infty)}{F_X(0)}[P]_0 \quad (2)$$

$$[P]_A = \frac{F_X(0) - F_X(\infty)}{F_X(0)}\frac{[L]_D}{[L]_A}[P]_0 \quad (3)$$

$[P]_0$ and $([L]_D/[L]_A)$ represent the initial concentration of the helix in the donor vesicles and the donor-to-acceptor lipid concentration ratio, respectively.

Calculation of the Transfer Free Energy. Our previous studies have suggested that in both the donor and acceptor vesicles a fraction of the helices also exists as an antiparallel dimer.[18] The concentration of monomer in each membrane [M] was calculated from the total peptide concentration [P] and the monomer−dimer association constant K_a obtained in the self-association experiments (vide infra):

$$[M] = \frac{\sqrt{8K_a[P] + 1} - 1}{4K_a} \quad (4)$$

$[M]_A/[M]_D$ gives the partition coefficient of the helix monomer from the donor to the acceptor. To precisely determine the partition coefficient of the peptide between the acceptor species Y

dx.doi.org/10.1021/bi200560c | *Biochemistry* 2011, 50, 6806−6814

and POPC, $K_{t(monomer)}^{POPC\rightarrow Y}$, we also used pure POPC vesicles as the acceptor vesicles in each experiment, to obtain $[M]_{POPC}$ values.

$$K_{t(monomer)}^{POPC\rightarrow Y} = \frac{[M]_Y}{[M]_{POPC}} \quad (5)$$

The free energy of transfer of the monomer from POPC to Y was calculated as

$$\Delta G_{t(monomer)}^{POPC\rightarrow Y} = -RT \ln K_{t(monomer)}^{POPC\rightarrow Y} \quad (6)$$

The corresponding ΔG_t value for the helix dimer was determined by

$$\Delta G_{t(dimer)}^{POPC\rightarrow Y} = -\Delta G_a^{POPC} + 2\Delta G_{t(monomer)}^{POPC\rightarrow Y} + \Delta G_a^{Y} \quad (7)$$

ΔG_a^{POPC} and ΔG_a^{Y} denote the Gibbs free energy for the formation of the antiparallel dimer in POPC and Y, respectively (vide infra).

Helix Self-Association. The self-association of the helix was determined by the FRET between **I** and **II**.[18] LUVs containing **I** and **II** were prepared, and the donor fluorescence (excitation and emission at 450 and 530 nm, respectively) was compared with that of the LUV without the acceptor in duplicate, after subtracting the background scattering of vesicles. The **I**/**II** ratio was kept at around 1/0.4 because this gave a sufficient fluorescence intensity of **I**, a larger signal change by the dimerization, and a smaller random (spontaneous) FRET.

FRET efficiency (E_T) or relative quantum yield ($Q_r = 1 - E_T$) was determined by the degree of NBD (donor) fluorescence quenching. E_T was calculated with

$$E_T = 1 - Q_r = 1 - (F_{DA}/F_D)([D]_D^{+MeOH}/[D]_{DA}^{+MeOH}) \quad (8)$$

F_{DA} and F_D denote the donor fluorescence intensity with and without the acceptor, respectively. $[D]_{DA}^{+MeOH}$ and $[D]_D^{+MeOH}$ express donor concentrations determined after the methanol solubilization.

The calculation of association free energy was described in ref 18. First, random FRET between a donor and randomly distributed acceptors was separated from FRET due to donor−acceptor association.

$$Q_r = (1 - f_b)q_s + f_b q_a \quad (9)$$

The fraction of donors associated with acceptors is denoted by f_b. Relative quantum yields due to random transfer and association are expressed by q_s and q_a, respectively. The q_s value was estimated based on the analysis of Wolber and Hudson.[23] The dimer fraction (f_d) can be calculated assuming a monomer−dimer equilibrium and a binomial distribution of donors and acceptors in the dimer.

$$f_d = \frac{f_b}{1 - P_d} \quad (10)$$

P_d denotes the fraction of donor in the donor−acceptor mixture. The association constant (K_a) and corresponding standard Gibbs free energy change (ΔG_a) are given by

$$\Delta G_a = -RT \ln K_a \quad (11)$$

$$K_a = \frac{[D]}{[M]^2} \quad (12)$$

R and T represent the gas constant and the absolute temperature, respectively. [D] and [M] denote the mole fractions of dimer and monomer in the bilayers, respectively. The experiments were performed at sufficiently low peptide concentrations, expecting an ideal dilution regime.

$$[M] = (1 - f_d)\frac{2n_p}{2n_p + n_l} \quad (13)$$

$$[D] = \frac{f_d n_p}{2n_p + n_l} \quad (14)$$

$$X_p = [M] + 2[D] = \frac{2n_p}{2n_p + n_l} \quad (15)$$

The moles of peptide and lipid are denoted by n_p and n_l, respectively. The total peptide mole fraction is represented by X_p. The factor of 2 was introduced to take the transmembrane nature of the peptide into consideration.

RESULTS

Partitioning of Peptides between Membranes. We first screened for lipid compositions that significantly affect the membrane partitioning of **I** by monitoring the intervesicular transfer of the peptide from POPC LUVs doped with 2 mol % Rh-PE (donor vesicles) to acceptor vesicles composed of various lipids. The intervesicular transfer proceeds via slow dissociation of the peptide into the aqueous phase and redistribution between vesicles, rather than via contact between vesicles.[20] As shown in Figure 1A, the transfer of the peptide from the donor to the acceptor vesicles resulted in a decrease in the sensitized emission from rhodamine accompanied by an increase in the emission from NBD. We confirmed that the transfer of headgroup-labeled lipids (Rh-PE and NBD-PE) was negligible in the time range (Figure 1A), although in general fluorophore-labeled lipids can transfer among vesicles with rates depending on the type of fluorophore, labeling position, and lipid composition.[24,25] The relative rhodamine fluorescence intensity, which linearly depends on the concentration of the peptide in the donor vesicles,[19] was monitored at 37 °C for acceptor membranes composed of POPC, 1-palmitoyl-2-oleoyl-*sn*-glycero-3-phosphatidylglycerol (POPG), 1-palmitoyl-2-oleoyl-*sn*-glycero-3-phosphatidylserine (POPS), and POPC/POPE (1/1) (Figure 1B). Membranes composed of negatively charged lipids (POPS and POPG) incorporated the peptides similarly to POPC membranes. On the other hand, POPE/POPC (1/1) membranes, which are zwitterionic but have a higher lateral pressure in the hydrocarbon core region, significantly decreased partitioning of the peptide. Furthermore, gel phase membranes (dimyristoyl-*sn*-glycero-3-phosphatidylcholine (DMPC) at 15 °C) completely excluded the peptide even after a 150 h incubation although the peptide slowly dissociated from donor vesicles even at this lower temperature, as confirmed by the transfer to acceptor membranes composed of POPC (Figure 1C). From the plateau values for exponential fitting ($F_X(\infty)$), the apparent transfer free energy from POPC to acceptor membranes was calculated at 37 °C as $\Delta G_t = -RT \ln (1 - F_X(\infty))/(1 - F_{POPC}(\infty))$ (Figure 1D). Even in the L_d phase, the partitioning to PC membranes with saturated acyl chains (DMPC at 37 °C) (ΔG_t = 0.5 ± 0.1 kJ mol^{-1}) was slightly decreased compared to that to dipalmitoleoyl-*sn*-glycero-3-phosphatidylcholine (DPoPC) having doubly monounsaturated acyl chains (ΔG_t = 0.2 ± 0.2 kJ mol^{-1}) despite similar hydrophobic thicknesses (~23 Å[26]). Among the membranes examined, however, an obvious effect was observed only for POPC/POPE (1/1) (ΔG_t = 4.6 ± 0.2 kJ mol^{-1}).

dx.doi.org/10.1021/bi200560c | *Biochemistry* 2011, 50, 6806−6814

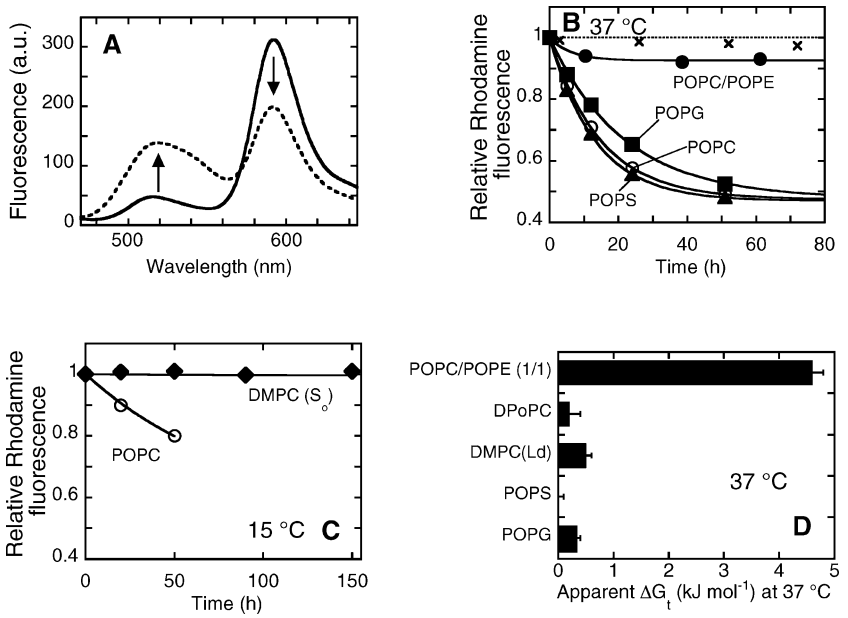

Figure 1. Measurement of the intervesicular transfer of the peptide. (A) An example of change in emission spectra upon intervesicular transfer of **I**. Donor POPC vesicles containing 0.5 mol % **I** and 2 mol % Rh-PE were incubated with acceptor DOPC vesicles at a donor-to-acceptor lipid ratio of 1:5 (total lipid concentration, 1.2 mM). NBD and rhodamine emission maxima were around 530 and 590 nm, respectively. Emission spectra before (solid trace) and after (dotted trace) a 51 h incubation at 37 °C are shown. (B) Time courses of sensitized rhodamine fluorescence intensity for acceptor vesicles composed of POPC (○), POPG (■), POPS (▲), and POPC/POPE (1/1) (●) at 37 °C. The transfer of fluorophore-labeled lipids (×) was also examined by incubating donor POPC vesicles containing 0.5 mol % NBD-PE and 2 mol % Rh-PE with acceptor POPC vesicles. (C) Time courses for POPC (○) and DMPC (◆) acceptor vesicles at 15 °C (n = 2). The observed values were fitted by the single-exponential function $F_x(t) = F_x(\infty) + (F_x(0) - F_x(\infty))\exp(-kt)$ as shown by lines. (D) Summary of apparent transfer free energies for various acceptor membranes at 37 °C (n = 2).

A reciprocal experiment, in which the peptide was transferred from donor POPC/POPE vesicles to acceptor POPC vesicles, gave a similar ΔG_t value with opposite sign ($\Delta G_t = -4.2 \pm 0.7$ kJ mol^{-1}, Supporting Information Figure S1), demonstrating that the system is reaching equilibrium.

FTIR-PATR. Our previous study has shown that the peptide $(AALALAA)_3$ assumed a stable transmembrane helix in PC bilayers even under hydrophobic mismatch conditions.[18] However, higher lateral pressure in the hydrocarbon core region induced by POPE may inhibit the transmembrane insertion of the helix. To examine the secondary structure and orientation of the peptide in POPC/POPE bilayers, we measured FTIR-PATR spectra of oriented bilayers containing 0.5 mol % peptides. Figure 2 shows the amide region spectra (1500−1700 cm^{-1}) for polarized light parallel and perpendicular to the plane of incidence measured at 25 °C. Narrow amide I and amide II absorption bands with half-widths of ~15 cm^{-1} were observed at around 1660 and 1547 cm^{-1}, respectively, characteristic for helices in both POPC and POPC/POPE membranes. Similar narrow peaks were observed at 5 and 55 °C (data not shown), indicating stable helical structures in the range of temperatures examined. The spectra including OD stretching (~2500 cm^{-1}) and lipid carbonyl (~1740 cm^{-1}) stretching bands are shown in Supporting Information Figure S2. The average orientation angle of the helix axis with respect to bilayer normal was estimated from R values for the amide I band assuming a fixed angle between the helix axis and direction of the transition dipole moment (see Experimental Procedures). The large R values (>3.8) indicate transmembrane orientations of the helices with orientation angles <30°. In general, the helices appeared to slightly tilt in the presence of PE (for example, R decreased from 6.4 to 4.3

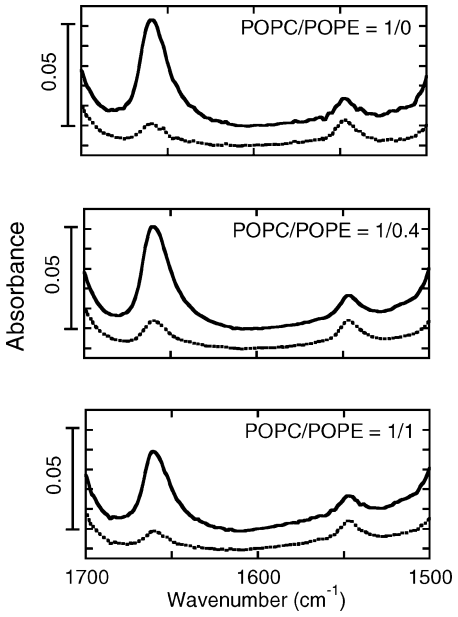

Figure 2. PATR-FTIR spectra in the amide region measured for **I**/lipid (1/200) films hydrated with D_2O (25 °C). The lipid compositions are shown in the figure. Solid and dotted lines indicate raw speactra for the IR beam with its electric vector parallel and perpendicular to the plane of incidence, respectively.

on incorporation of 50% POPE at 25 °C). The amide I/amide II absorption ratios calculated from unpolarized spectra[18] were similar in POPC and POPC/POPE bilayers (~3.0, data not shown), suggesting that the helix was embedded in the hydrocarbon core of the membrane without H/D exchange.[27]

dx.doi.org/10.1021/bi200560c | Biochemistry 2011, 50, 6806−6814

We concluded that the helices assume transmembrane orientations in both POPC and POPC/POPE bilayers.

Formation of Antiparallel Dimer. Our previous studies have demonstrated that the helix preferentially associated in an antiparallel orientation at low concentrations because of electrostatic interaction between helix macrodipoles.[18,22] At higher concentrations, the formation of a parallel dimer and/or higher oligomers resulted in the self-quenching of the fluorescent probe NBD placed at the N-terminus of the peptide. To determine the concentration range for measurement of the equilibrium between the monomer and antiparallel dimer, the concentration dependence of the NBD fluorescence of **I** was measured in POPC and POPC/POPE (1/1) membranes (Supporting Information Figure S3). The concentration up to which the fluorescence increases linearly was determined to be X_p = 0.02 and 0.0022 in POPC and POPC/POPE vesicles, respectively. To detect the antiparallel dimer by FRET, the fluorescence donor NBD and the nonfluorescent acceptor DABMI were attached at the N- and C-terminus of the peptide, respectively (**I** and **II**). Fluorescence spectra for **I** were measured in the absence and presence of **II** (Figure 3).

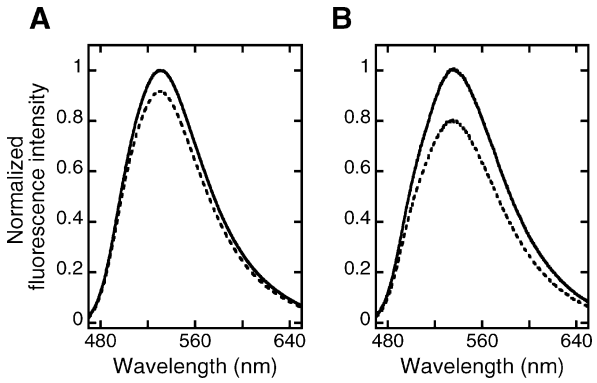

Figure 3. Examples of fluorescence spectra for **I** in the absence (solid line) and presence (dotted line) of nonfluorescent quencher **II** incorporated into (A) POPC and (B) POPC/POPE = 1/1 vesicles at 25 °C. The peptide mole fraction (X_p), **I**/**II** ratio, and lipid concentration were 0.0012, 1/0.4, and 50 μM, respectively. Slight differences in the concentration of **I** between samples were corrected (see eq 8).

We assumed that the fluorescence of NBD is completely quenched in the antiparallel heterodimer composed of **I** and **II** (q_a = 0).[18] Contribution from the random FRET originating from the random distribution of the acceptor (<5%) was subtracted to analyze the FRET from the dimer (see Experimental Procedures). Even at the smallest X_p value, 0.0012, a significant FRET was observed in POPC/POPE bilayers (Figure 3B). Note that the minimal F_{DA}/F_D value corresponding to complete dimerization is ~0.6.

Figure 4 plots the dimer fraction as a function of X_p in the temperature range 15−55 °C. The concentration dependence of dimerization well fitted the theoretical curve assuming a monomer−dimer equilibrium with the association constant K_a as the adjustable parameter.

$$f_d = \frac{4K_aX_p + 1 - \sqrt{8K_aX_p + 1}}{4K_aX_p} \quad (16)$$

Energetics of Partitioning and Self-Association. Based on the above measurements, thermodynamic parameters for intermembrane transfer and the formation of the antiparallel

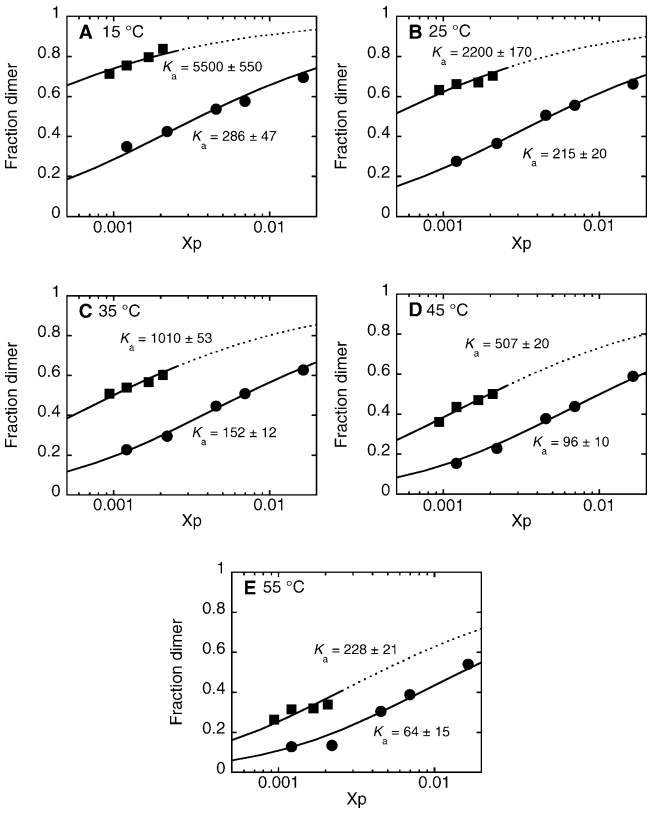

Figure 4. Monomer−dimer equilibrium of the helix in POPC (●) and POPC/POPE (1/1) (■) bilayers measured at (A) 15 °C, (B) 25 °C, (C) 35 °C, (D) 45 °C, and (E) 55 °C (n = 2). Error bars are within the symbols. Solid lines indicate fitting curves assuming a monomer−dimer equilibrium (eq 16) with K_a values indicated in the figure.

dimer were calculated as described in Experimental Procedures. Here transfer energies for the monomer and dimer were determined separately by considering association constants in the donor and acceptor vesicles (Figure 5A). Intermembrane

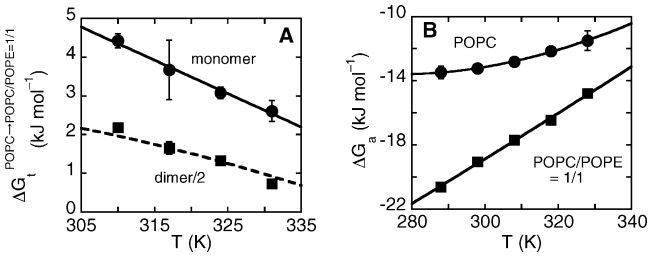

Figure 5. Temperature dependence of (A) ΔG_t and (B) ΔG_a. Solid lines indicate fitting using eq 17 assuming $\Delta C_{p(a)}$ = 0 except for ΔG_a in POPC vesicles. In the case of $\Delta G_{t(dimer)}$, a theoretical curve (dotted line) was reproduced from the thermodynamic parameters in Table 1.

partitioning of the helix from POPC to POPC/POPE (1/1) was generally unfavorable up to 4.5 kJ mol^{-1} in the experimental conditions, and the tendency was stronger at lower temperatures and for the monomer. Formation of the antiparallel dimer, however, was facilitated in the presence of POPE and at lower temperatures down to −22 kJ mol^{-1} (Figure 5B). The temperature dependence of the thermodynamic parameters for

dx.doi.org/10.1021/bi200560c | Biochemistry 2011, 50, 6806−6814

the transfer and self-association was analyzed using eq 17[18,28]

$$\Delta G = \Delta H + \Delta C_p(T - T_{ref}) - T\Delta S - T\Delta C_p \ln(T/T_{ref}) \quad (17)$$

T and T_{ref} represent the observed temperature and the standard-state reference temperature (308 K in this study), respectively. The data were adequately fitted by linear regression ($\Delta C_p = 0$) for the transfer and self-association in POPC/POPE (1/1), indicating that the changes in enthalpy and entropy are temperature-independent, whereas a deviation from linearity was observed for self-association in POPC. In the latter case, a nonzero ΔC_p value was assumed for the fitting. In the case of the transfer of the dimer, the thermodynamic parameters were indirectly determined from those for the transfer of the monomer and dimerization (eq 7). The thermodynamic parameters ΔH, $-T\Delta S$, and ΔC_p at 308 K for transfer and association are summarized in Tables 1 and 2, respectively. The transfer from POPC to POPC/POPE membranes was unfavorable because of significant increases in enthalpy for the monomer (+31.1 ± 2.1 kJ mol^{-1}) and dimer (+14.5 ± 1.6 kJ mol^{-1}), which are largely compensated for by decreases in entropic term (−26.5 ± 2.0 and −12.4 ± 1.6 kJ mol^{-1} for the monomer and dimer, respectively). On the other hand, formation of the antiparallel dimer in POPC/POPE bilayers was driven by a significant decrease in enthalpy (−61.5 ± 1.4 kJ mol^{-1}), accompanied by an increase in entropic term (+43.8 ± 1.5 kJ mol^{-1}).

DISCUSSION

In this study, we demonstrated a significant effect of POPE on the fundamental processes for membrane protein folding, i.e., insertion and self-association of transmembrane helices, through measurements of thermodynamic parameters using a model transmembrane helix $(AALALAA)_3$. Considering the inert character of the helix consisting of only hydrophobic residues (Leu and Ala) without flanking hydrophilic or aromatic residues, it is reasonable to assume that (1) the observed effect of lipid composition on the behavior of transmembrane helices represents a basal property of the transmembrane helix and (2) the effect primarily originates from the difference in physical properties of the bilayers, rather than from the difference in specific interactions between the helices and lipid headgroups (PC or PE).

Transmembrane Structure. Our FTIR measurements demonstrated that the peptide forms a stable helical secondary structure with a transmembrane orientation (orientation angle <25°) in PE-containing bilayers. The highly stable secondary structure of the helix in PE-containing membranes is consistent with other study using another model transmembrane helix, K_2-$(LA)_{12}$-K_2, although the structure can be disrupted in gel phase.[29] In the presence of POPE, a larger orientation angle of the helix was observed. However, surface binding of the helix at the water−membrane interface is not plausible because of (1) the absence of amphiphilicity in the helix and (2) no H/D exchange of backbone amide protons, although such an interfacial orientation should exist as a metastable state in the membrane insertion process.[20a] We considered that the observed larger orientation angle was due to the formation of transmembrane helix dimers with a larger crossing angle in PE-containing bilayers (vide infra).

Membrane Partitioning. The intervesicular transfer experiments revealed a significant enthalpy-driven, inhibitory effect of PE on the membrane partitioning of the transmembrane helix. For the helix monomer, electrostatic energy for burying the partial charge of the helix macrodipole would be unfavorable in thicker membranes because of lower dielectric constants around the helix termini, as discussed in our previous study under hydrophobic mismatch conditions.[19] PE lipids with a smaller headgroup increase the hydrophobic thickness of the bilayers by ordering acyl chains to compensate for the reduced headgroup repulsions. Recent deuterium NMR experiments suggest that a difference in hydrophobic thickness between POPC bilayers (~26.9 Å) and POPE bilayers (~29.1 Å) is 2.2 Å.[30] We assumed that the hydrophobic thickness of POPC/POPE (1/1) bilayers was their average (28.0 Å). Assuming a helix length of 27.5 Å,[18] the dielectric constant at the helix termini is expected to decrease from ~15 to ~10 upon transfer from POPC to POPC/POPE (1/1) bilayers.[31] The corresponding increase in enthalpic Born energy is only ~8 kJ mol^{-1}, which is much smaller than the observed ΔH_t value (31 kJ mol^{-1}). It should be noted that a stronger hydration of the headgroup region in PE-containing bilayers[32] can further attenuate the difference in Born energy. The remaining unfavorable enthalpy (>23 kJ mol^{-1}) can be attributed to the stronger lipid−lipid packing (or higher lateral pressure) in the hydrocarbon core region in PE-containing bilayers, originating from a decrease in headgroup repulsion.[33,34] The favorable change in the entropic term ($-T\Delta S_t$ = −27 kJ mol^{-1}) is also consistent with the stronger packing and ordering of lipid acyl chains in PE-containing bilayers.

Here we introduce a lattice-like model to clarify the differences in the number of molecular contacts upon the transfer.[18] The transfer can be expressed using the differential helix−lipid and lipid−lipid interaction free energy assuming k

Table 1. Thermodynamic Parameters for Transfer of the Helix from POPC (X) to POPC/POPE (1/1) (Y) at 308 K

	$\Delta G_t^{X\to Y}$ (kJ mol^{-1})	$\Delta H_t^{X\to Y}$ (kJ mol^{-1})	$-T\Delta S_t^{X\to Y}$ (kJ mol^{-1})	$\Delta C_{p(t)}^{X\to Y}$ (J K^{-1} mol^{-1})
monomer[a]	+4.5 ± 2.9	+31.1 ± 2.1	−26.5 ± 2.0	
dimer/2[b]	+2.1 ± 2.3	+14.5 ± 1.6	−12.4 ± 1.6	+0.2 ± 0.1

[a]Estimated assuming $\Delta C_{p(t)} = 0$. [b]Thermodynamic parameters were determined using eq 7.

Table 2. Thermodynamic Parameters for the Formation of the Antiparallel Dimer of the Helix at 308 K

membranes	ΔG_a (kJ mol^{-1})	ΔH_a (kJ mol^{-1})	$-T\Delta S_a$ (kJ mol^{-1})	$\Delta C_{p(a)}$ (J K^{-1} mol^{-1})
POPC (X)	−12.8 ± 0.2	−28.3 ± 0.4	+15.5 ± 0.4	−0.5 ± 0.1
POPC/POPE (1/1) (Y)[a]	−17.7 ± 0.1	−61.5 ± 1.4	+43.8 ± 1.5	

[a]Estimated assuming $\Delta C_{p(a)} = 0$.

dx.doi.org/10.1021/bi200560c | Biochemistry 2011, 50, 6806−6814

lipids around one helix (~12)

$$\Delta G_{t(monomer)}^{X\rightarrow Y} = -\frac{k}{2}\Delta\Delta G_{L-L}^{X\rightarrow Y} + k\Delta\Delta G_{H-L}^{X\rightarrow Y} \quad (18)$$

where X = POPC and Y = POPC/POPE (1/1)). A similar analysis is possible for ΔH_t and ΔS_t. Assuming that the helix monomer−lipid interactions are similar in POPC and POPC/POPE bilayers having the same acyl chains except the Born energy ($k\Delta\Delta H_{H-L}$ = 8 kJ mol^{-1}), $\Delta\Delta H_{L-L}$ and $\Delta\Delta S_{L-L}$ are estimated to be −4 kJ mol^{-1} and −14 J mol^{-1} K^{-1}, respectively (eq 18). The observed differences were almost twice those for fluid-to-gel phase transition per CH_2 group (ΔH = −2.1 kJ mol^{-1} and ΔS = −5.6 J mol^{-1} K^{-1},[35] in accordance with the hypothesis that they originated from differential lipid−lipid interactions). The transfer free energy for the dimer was less unfavorable with a weaker enthalpy/entropy compensation than that for the monomer because (1) the antiparallel dimer partially neutralizes the terminal charges from helix macrodipole, decreasing the unfavorable Born energy, and (2) better protein−lipid packing in PE-containing bilayers by dimerization (vide infra).

Formation of the Antiparallel Dimer. The energetic contributions from helix−helix interactions were estimated using the lattice model, assuming that the formation of a new helix−helix contact accompanies a decrease and increase in helix−lipid and lipid−lipid contacts, respectively.[4,18,36] Considering the differencial free energy of association between the two lipid systems

$$\begin{aligned}\Delta G_a^Y - \Delta G_a^X &\equiv \Delta\Delta G_a^{X\rightarrow Y}\\ &= \Delta\Delta G_{H-H}^{X\rightarrow Y} + \frac{n}{2}\Delta\Delta G_{L-L}^{X\rightarrow Y}\\ &\quad - n\Delta\Delta G_{H-L}^{X\rightarrow Y}\end{aligned} \quad (19)$$

Here n is the number of lipids removed from the vicinity of the helix to bulk lipids upon the association (~4).[18] Thermodynamic parameters for helix−helix interaction were calculated by combining eqs 18 and 19

$$\begin{aligned}\Delta\Delta G_{H-H}^{X\rightarrow Y} &= \Delta\Delta G_a^{X\rightarrow Y} - \frac{n}{2}\Delta\Delta G_{L-L}^{X\rightarrow Y}\\ &\quad + n\Delta\Delta G_{H-L}^{X\rightarrow Y}\\ &= \Delta\Delta G_a^{X\rightarrow Y} + \frac{n}{k}\Delta G_{t(monomer)}^{X\rightarrow Y}\end{aligned} \quad (20)$$

The observed stronger self-association in PE-containing vesicles ($\Delta\Delta G_a$ = −4.9 kJ mol^{-1}) originates not only from direct helix−helix interactions ($\Delta\Delta G_{H-H}$ = −3.4 kJ mol^{-1}) but also from indirect lipid−lipid ($n\Delta\Delta G_{L-L}/2$) and helix−lipid ($-n\Delta\Delta G_{H-L}$) interactions. A similar analysis of the $\Delta\Delta H_a$ and $-T\Delta\Delta S_a$ terms indicates that the helix−helix interaction and the other interactions were enthalpy-driven and similar in magnitude ($\Delta\Delta H_{H-H}$ = −23 kJ mol^{-1} and $n\Delta\Delta H_{L-L}/2 - n\Delta\Delta H_{H-L}$ = −10 kJ mol^{-1}). Interestingly, the PE-induced forces were enthalpically favorable, in contrast to conventional hydrophobic interactions in aqueous phase, which is entropy-driven. Similarly to the discussion of the helix transfer (vide supra), the latter contribution ($n\Delta\Delta H_{L-L}/2 - n\Delta\Delta H_{H-L}$) predominantly reflects the differences in lipid−lipid interactions in the hydrocarbon core region ($n\Delta\Delta H_{L-L}/2$ ~ −8 kJ mol^{-1}). The observed difference in enthalpy change for helix−helix interactions (−23 kJ mol^{-1}) was only partially explained by an increase in electrostatic interaction between helix macrodipoles (−8 kJ mol^{-1}) calculated as described in ref 18 (see also Supporting Information Figure S5) assuming a change in crossing angle between the helices (ϕ, POPC: ~0°; POPC/POPE: 44°, calculated from the dichroic ratios at 25 °C) and a decrease in dielectric constants at the helix termini from 15 to 8 (membrane thickening and helix tilting). Helix−helix contact in an hourglass-shape with a crossing angle can partially compensate for the negative curvature strain (or higher lateral pressure in hydrocarbon core) of PE-containing bilayers. This lipid reorganization effect upon dimerization in POPC/POPE bilayers, inherent helix−lipid interactions, is incorporated in the H−H term in the lattice model (eq 20). Dan and Safran calculated excess energy originating from the lateral pressure profile as a form of line tension on transmembrane proteins, based on physical properties of monolayers (spontaneous curvature and elasticity) and proteins (contact angle between the monolayer and the protein).[37] The line tension on the helix dimer in POPC/POPE and POPC bilayers was calculated according to the model (eq 3b in ref 37) assuming the contact angles (POPC: ~0°; POPC/POPE: 22°) and membrane physicochemical parameters.[38,39b] A significant decrease in tension (0.24 kJ mol^{-1} Å^{-1}) in POPC/POPE bilayers compared with that in POPC bilayers was estimated, which is comparable to the observed favorable $\Delta\Delta H_{H-H}$ other than from stronger helix macrodipole interaction (−15 kJ mol^{-1}) considering that the lipid-accessible circumference is ~60 Å, although the numerical value of the tension was sensitive to the contact angle. The favorable protein−lipid packing upon dimerization in PE-containing bilayers is also consistent with the observed unfavorable change in entropic term ($-T\Delta\Delta S_{H-H}$ = +19 kJ mol^{-1}). Another factor that can affect the difference in the entropic term is changes in the hydrophobic interaction near the helix termini.[18] In addition to the above interactions, long-range and generally nonmonotonic interactions such as lipid-mediated protein−protein interaction[40,41] originating from the oscillating fluctuation of carbon density around a protein may also contribute to stronger helix−helix interactions in PE-containing membranes. A theoretical study performed by Bohonc and co-workers based on membrane elasticity theory and director model predicts attractive helix−helix interactions in bilayers with a negative spontaneous curvature, which is significantly enhanced in negative hydrophobic mismatch conditions (thicker bilayers compared with the length of the helix).[41]

$\Delta C_{p(a)}$ was negative in POPC bilayers, whereas it was ~0 in POPC/POPE bilayers. ΔC_p has been considered a hallmark of hydrophobic interactions.[42,43] Hourglass-shaped dimers formed in PE-containing bilayers may increase the penetration by water of the hydrophobic region, which increases $\Delta C_{p(a)}$.

In contrast to our results, the self-association of a poly-leucine-based model transmembrane helix ($K_2GL_7WL_9K_2A$) was not enhanced in DOPC/DOPE bilayers compared with that in DOPC bilayers.[44] Differences in the design of the helix appear to result in the striking difference in response to incorporation of PE. The flanking Lys residues can contribute to lateral pressure in the headgroup region, which can alter the response to change in the lateral pressure profile. Furthermore, electrostatic repulsion between Lys residues should significantly reduce self-association of the helix.

CONCLUSION

By using the above lattice-like model, the significant effects of POPE on the thermodynamics of membrane partitioning and oligomerization of the inert transmembrane helix have been well described as alterations in the balance among lipid−lipid, helix−lipid, and helix−helix interactions. For the transfer of the helix from PC to PC/PE membranes, the observed unfavorable enthalpy ΔH_t (+31 kJ mol^{-1}) can be attributed to a loss of strong lipid−lipid interaction (+23 kJ mol^{-1}) and more unfavorable helix−lipid interactions (the Born energy, +8 kJ mol^{-1} in the PE-containing membranes). The favorable enthalpy change upon dimerization of the helices $\Delta\Delta H_a$ (−33 kJ mol^{-1}) was roughly decomposed into a decrease in the number of helix−lipid contacts (the Born energy, −2 kJ mol^{-1}), stronger helix macrodipole interactions (−8 kJ mol^{-1}), increase in the number of lipid−lipid contacts (−8 kJ mol^{-1}), and difference in the strength of helix−lipid interactions between the monomer and dimer (−15 kJ mol^{-1}). The latter two driving forces, comprising ∼70% of $\Delta\Delta H_a$, originate from the lateral pressure profile in membranes and should represent a general "lipophobic" interaction on transmembrane helices, originally proposed in theoretical studies.[40,41,45,46] The above principle will generally work for interactions between nonbilayer-forming lipids and transmembrane helices. The lipophobic forces demonstrated in this study may be a regulatory mechanism for bilayer-dependent modulation of the folding and conformational equilibrium of membrane proteins.

ASSOCIATED CONTENT

Supporting Information

Time courses for reciprocal transfer, additional FTIR spectra, self-quenching of NBD-labeled helix, and schemes for dipole−dipole interaction. This material is available free of charge via the Internet at http://pubs.acs.org.

AUTHOR INFORMATION

Corresponding Author

*Tel: 81-75-753-4521. Fax: 81-75-753-4578. E-mail: katsumim@pharm.kyoto-u.ac.jp.

Funding

This work was supported in part by Grant-in-Aid for Scientific Research on Innovative Areas (21107514) and Encouragement of Young Scientists (B) (18790025) from the Ministry of Education, Culture, Sports, Science and Technology of Japan.

ABBREVIATIONS

DABMI, *n*-[4-[[4-(dimethylamino)phenyl]azo]phenyl]-4′-maleimide; DMPC, dimyristoyl-*sn*-glycero-3-phosphatidylcholine; DPoPC, dipalmitoleoyl-*sn*-glycero-3-phosphatidylcholine; FTIR-PATR, Fourier transform infrared-polarized attenuated total reflection; FRET, fluorescence resonance energy transfer; LUVs, large unilamellar vesicles; NBD, 7-nitrobenz-2-oxa-1,3-diazole; PC, phosphatidylcholine; NBD-PE, *N*-(7-nitrobenz-2-oxa-1,3-diazol-4-yl)-1,2-dihexadecanoyl-*sn*-glycero-3-phosphoethanolamine, triethylammonium salt; PE, phosphatidylethanolamine; POPC, 1-palmitoyl-2-oleoyl-*sn*-glycero-3-phosphatidylcholine; POPE, 1-palmitoyl-2-oleoyl-*sn*-glycero-3-phosphatidylethanoamine; POPG, 1-palmitoyl-2-oleoyl-*sn*-glycero-3-phosphatidylglycerol; POPS, 1-palmitoyl-2-oleoyl-*sn*-glycero-3-phosphatidylserine; Rh-PE, Lissamine Rhodamine B 1,2-dihexadecanol-*sn*-glycero-3-phosphatidylethanolamine, triethylammonium salt.

ADDITIONAL NOTES

[a]Helix self-association experiments in POPC/POPE (1/1) vesicles (Figure 4) suggest that most helices form a dimer or higher order oligomers under experimental conditions (X_P = 0.01). Therefore, the FTIR data do not directly support a transmembrane orientation for the helix monomer. However, we also observed a large *R* value (4.5) for the amide I band even at a lower peptide concentration (X_P = 0.003) at 55 °C (Supporting Figure S4), at which ∼60% of the helices should exist as monomers.

[b]Parameters used for POPC and POPC/POPE (1/1) monolayers respectively were as follows: area per lipid, 68.3 and 65.8 Å^2;[37] hydrophobic thickness, 13.45 and 14 Å;[28] lateral compressibility per lipid, 68.2 × 10^{-21} and 73.2 × 10^{-21} J (calculated from area expansion[36] and area per lipid[37]); bending modulus, 39.1 × 10^{-21} J (9.5 k_BT) and 42.2 × 10^{-21} J (10.3 k_BT);[37] spontaneous curvature normalized to monolayer thickness, 0 and −0.245.[37] The parameters for POPC/POPE monolayers were assumed to be the averages of those for SOPC and POPE[36] or POPC and DOPE.[37]

REFERENCES

(1) Haltia, T., and Freire, E. (1995) Forces and factors that contribute to the structural stability of membrane proteins. *Biochim. Biophys. Acta 1241*, 295−322.

(2) White, S. H., and Wimley, W. C. (1998) Hydrophobic interactions of peptides with membrane interfaces. *Biochim. Biophys. Acta 1376*, 339−352.

(3) Cornelius, F. (2001) Modulation of Na,K-ATPase and Na-ATPase activity by phospholipids and cholesterol. I. Steady-state kinetics. *Biochemistry 40*, 8842−8851.

(4) Lee, A. G. (2004) How lipids affect the activities of integral membrane proteins. *Biochim. Biophys. Acta 1666*, 62−87.

(5) van der Does, C., Swaving, J., van Klompenburg, W., and Driessen, A. J. (2000) Non-bilayer lipids stimulate the activity of the reconstituted bacterial protein translocase. *J. Biol. Chem. 275*, 2472−2478.

(6) Yang, F. Y., and Hwang, F. (1996) Effect of non-bilayer lipids on the activity of membrane enzymes. *Chem. Phys. Lipids 81*, 197−202.

(7) Botelho, A. V., Gibson, N. J., Thurmond, R. L., Wang, Y., and Brown, M. F. (2002) Conformational energetics of rhodopsin modulated by nonlamellar-forming lipids. *Biochemistry 41*, 6354−6368.

(8) Marsh, D. (2007) Lateral pressure profile, spontaneous curvature frustration, and the incorporation and conformation of proteins in membranes. *Biophys. J. 93*, 3884−3899.

(9) Cantor, R. S. (1997) Lateral pressures in cell membranes: a mechanism for modulation of protein function. *J. Phys. Chem. B 101*, 1723−1725.

(10) White, S. H., and Wimley, W. C. (1999) Membrane protein folding and stability: physical principles. *Annu. Rev. Biophys. Biomol. Struct. 28*, 319−365.

(11) Engelman, D. M., Chen, Y., Chin, C. N., Curran, A. R., Dixon, A. M., Dupuy, A. D., Lee, A. S., Lehnert, U., Matthews, E. E., Reshetnyak, Y. K., Senes, A., and Popot, J. L. (2003) Membrane protein folding: beyond the two stage model. *FEBS Lett. 555*, 122−125.

(12) Van den Berg, B., Clemons, W. M. Jr., Collinson, I., Modis, Y., Hartmann, E., Harrison, S. C., and Rapoport, T. A. (2004) X-ray structure of a protein-conducting channel. *Nature 427*, 36−44.

(13) Hessa, T., Meindl-Beinker, N. M., Bernsel, A., Kim, H., Sato, Y., Lerch-Bader, M., Nilsson, I., White, S. H., and von Heijne, G. (2007)

Molecular code for transmembrane-helix recognition by the Sec61 translocon. *Nature 450*, 1026−1030.

(14) White, S. H., and von Heijne, G. (2008) How translocons select transmembrane helices. *Annu. Rev. Biophys. Biomol. Struct. 37*, 23−42.

(15) Jaud, S., Fernandez-Vidal, M., Nilsson, I., Meindl-Beinker, N. M., Hubner, N. C., Tobias, D. J., von Heijne, G., and White, S. H. (2009) Insertion of short transmembrane helices by the Sec61 translocon. *Proc. Natl. Acad. Sci. U.S.A. 106*, 11588−11593.

(16) Mackenzie, K. R. (2006) Folding and stability of α-helical integral membrane proteins. *Chem. Rev. 106*, 1931−1977.

(17) Nyholm, T. K., Ozdirekcan, S., and Killian, J. A. (2007) How protein transmembrane segments sense the lipid environment. *Biochemistry 46*, 1457−1465.

(18) Yano, Y., and Matsuzaki, K. (2006) Measurement of thermodynamic parameters for hydrophobic mismatch 1: self-association of a transmembrane helix. *Biochemistry 45*, 3370−3378.

(19) Yano, Y., Ogura, M., and Matsuzaki, K. (2006) Measurement of thermodynamic parameters for hydrophobic mismatch 2: intermembrane transfer of a transmembrane helix. *Biochemistry 45*, 3379−3385.

(20) Yano, Y., and Matsuzaki, K. (2002) Membrane insertion and dissociation processes of a model transmembrane helix. *Biochemistry 41*, 12407−12413.

(21) Bartlett, G. R. (1959) Phosphorus assay in column chromatography. *J. Biol. Chem. 234*, 466−468.

(22) Yano, Y., Takemoto, T., Kobayashi, S., Yasui, H., Sakurai, H., Ohashi, W., Niwa, M., Futaki, S., Sugiura, Y., and Matsuzaki, K. (2002) Topological stability and self-association of a completely hydrophobic model transmembrane helix in lipid bilayers. *Biochemistry 41*, 3073−3080.

(23) Wolber, P. K., and Hudson, B. S. (1979) An analytic solution to the Förster energy transfer problem in two dimensions. *Biophys. J. 28*, 197−210.

(24) Nichols, J. W., and Pagano, R. E. (1982) Use of resonance energy transfer to study the kinetics of amphiphile transfer between vesicles. *Biochemistry 21*, 1720−1726.

(25) Silvius, J. R., and Leventis, R. (1993) Spontaneous interbilayer transfer of phospholipids: dependence on acyl chain composition. *Biochemistry 32*, 13318−13326.

(26) Lewis, B. A., and Engelman, D. M. (1983) Lipid bilayer thickness varies linearly with acyl chain length in fluid phosphatidylcholine vesicles. *J. Mol. Biol. 166*, 211−217.

(27) Goormaghtigh, E., Raussens, V., and Ruysschaert, J. M. (1999) Attenuated total reflection infrared spectroscopy of proteins and lipids in biological membranes. *Biochim. Biophys. Acta 1422*, 105−185.

(28) Russell, C. J., Thorgeirsson, T. E., and Shin, Y. K. (1996) Temperature dependence of polypeptide partitioning between water and phospholipid bilayers. *Biochemistry 35*, 9526−9532.

(29) Zhang, Y. P., Lewis, R. N., Hodges, R. S., and McElhaney, R. N. (2001) Peptide models of the helical hydrophobic transmembrane segments of membrane proteins: interactions of acetyl-K_2-$(LA)_{12}$-K_2-amide with phosphatidylethanolamine bilayer membranes. *Biochemistry 40*, 474−482.

(30) Salnikov, E. S., Mason, A. J., and Bechinger, B. (2009) Membrane order perturbation in the presence of antimicrobial peptides by ^{2}H solid-state NMR spectroscopy. *Biochimie 91*, 734−743.

(31) Mazeres, S., Schram, V., Tocanne, J. F., and Lopez, A. (1996) 7-nitrobenz-2-oxa-1,3-diazole-4-yl-labeled phospholipids in lipid membranes: differences in fluorescence behavior. *Biophys. J. 71*, 327−335.

(32) Shintou, K., Nakano, M., Kamo, T., Kuroda, Y., and Handa, T. (2007) Interaction of an amphipathic peptide with phosphatidycholine/phosphatidylethanolamine mixed membranes. *Biophys. J. 93*, 3900−3906.

(33) Gruner, S. M. (1985) Intrinsic curvature hypothesis for biomembrane lipid composition: a role for nonbilayer lipids. *Proc. Natl. Acad. Sci. U.S.A. 82*, 3665−3669.

(34) van den Brink-van der Laan, E., Killian, J. A., and de Kruijff, B. (2004) Nonbilayer lipids affect peripheral and integral membrane proteins via changes in the lateral pressure profile. *Biochim. Biophys. Acta 1666*, 275−288.

(35) Seddon, J.M., Cevc, G., and Marsh, D. (1983) Calorimetric studies of the gel-fluid (L_β-L_α) and lamellar-inverted hexagonal (L_α-H_{II}) phase transitions in dialkyl- and diacylphosphatidylethanolamines. *Biochemistry 22*, 1280−1289.

(36) Lemmon, M. A., and Engelman, D. M. (1994) Specificity and promiscuity in membrane helix interactions. *Q. Rev. Biophys. 27*, 157−218.

(37) Dan, N., and Safran, S. A. (1998) Effect of lipid characteristics on the structure of transmembrane proteins. *Biophys. J. 75*, 1410−1414.

(38) Evans, E., and Needham, D. (1987) Physical properties of surfactant bilayer membranes: thermal transitions, elasticity, rigidity, cohesion, and colloidal interactions. *J. Phys. Chem. 91*, 4219−4228.

(39) Soubias, O., Teague, W. E. Jr., Hines, K. G., Mitchell, D. C., and Gawrisch, K. (2010) Contribution of membrane elastic energy to rhodopsin function. *Biophys. J. 99*, 817−824.

(40) Lague, P., Zuckermann, M. J., and Roux, B. (2001) Lipid-mediated interactions between intrinsic membrane proteins: dependence on protein size and lipid composition. *Biophys. J. 81*, 276−284.

(41) Bohonc, K., Kralj-Iglic, V., and May, S. (2003) Interaction between two cylindrical inclusions in a symmetric lipid bilayer. *J. Chem. Phys. 119*, 7435−7444.

(42) Baldwin, R. L. (1986) Temperature dependence of the hydrophobic interaction in protein folding. *Proc. Natl. Acad. Sci. U.S.A. 83*, 8069−8072.

(43) Wimley, W. C., and White, S. H. (1993) Membrane partitioning: distinguishing bilayer effects from the hydrophobic effect. *Biochemistry 32*, 6307−6312.

(44) Mall, S., Broadbridge, R., Sharma, R. P., East, J. M., and Lee, A. G. (2001) Self-association of model transmembrane α-helices is modulated by lipid structure. *Biochemistry 40*, 12379−12386.

(45) Owicki, J. C., Springgate, M. W., and McConnell, H. M. (1978) Theoretical study of protein−lipid interactions in bilayer membranes. *Proc. Natl. Acad. Sci. U.S.A. 75*, 1616−1619.

(46) Jahnig, F. (1983) Thermodynamics and kinetics of protein incorporation into membranes. *Proc. Natl. Acad. Sci. U.S.A. 80*, 3691−3695.